Shallow Angle Wave Profiling Lidar

M. R. BELMONT, J. M. K. HORWOOD, R. W. F. THURLEY, AND J. BAKER

School of Engineering, Computer Science and Mathematics, University of Exeter, Devon, United Kingdom

(Manuscript received 10 May 2006, in final form 23 August 2006)

ABSTRACT

A lidar scanning system is described that is primarily designed to measure sea wave shape. The device is capable of measuring real-time spatial profiles over distances of hundreds of meters, and as the lidar must inevitably operate from modest elevations (e.g., from a vessel's masthead), it is inherently a very shallow angle metrology device. This results in a highly nonuniform distribution of the wave elevation values. The vertical and horizontal resolution is primarily set by the characteristics of the optical system employed and range/data capacity is set by signal-to-noise ratio considerations. Illustrative data are presented as consecutive profiles taken 0.2 s apart for highly trochoidal waves under conditions where the height was recorded to ±0.03 m and horizontal sample separation to ±0.025 m. A comparison is presented with traditional wave staff measurements.

1. Background

This research note briefly introduces a new approach to wave measurements based upon shallow angle lidars and highlights new metrology issues specific to the method. The technique is capable of measuring the time evolution of spatial profiles of sea waves over an extended region of several hundred meters for effectively unlimited periods of time.

The measurement of time-resolved spatial profiles of propagating sea waves has obvious applications in fundamental wave research and in addition has very practical uses in areas as diverse as improved understanding of beach erosion mechanisms (Gallagher et al. 1998; Lee et al. 1998; Jackson 1999), short-term prediction of swell waves aimed at predicting wave-induced motion of large vessels (Morris et al. 1992, 1998), and identification of the initial conditions associated with extreme waves (Clauss 2001). Experimentally, such data are difficult to acquire. The classical Stereo Wave Observation Project (SWOP) experiment (Cote et al. 1960) is unrealistic as a routine method and the large arrays of traditional wave sensors required for such a task are expensive and immobile. To be of practical value, a wave profile measurement system requires some form of a portable remote sensing device.

Long wavelength radars provide statistical sea surface roughness measures and wave direction (Tucker 1991), but not spatial profiles. Shortwave radars can fulfill the same role and their reduced wavelength would suggest that spatial profiling might also be possible. The performance of any active electromagnetic remote probe beam–based sensing system is controlled by the fundamental resolution restriction defined by the ratio (wavelength/aperture). A consequence of this is that for airborne "look down" radars, the achievable radar beamwidths provide adequate resolution for sea surface profiling. However, airborne measurement systems suffer from the following problems: (i) they are expensive to operate, (ii) they provide limited data availability, and (iii) typical deployment from fixed wing aircraft means they are unable to observe wave evolution over a fixed spatial region. At present, satellite data also cannot achieve the desired resolution. For continuous low-cost observation, either shore- or vessel-based instruments are required.

Unless such surface-based systems are restricted to very local measurements they will inevitably be operating at shallow angles as suggested in Fig. 1, and for shipborne work observing deep-water sea waves, a combination of factors mean that the angles are often as small as 5°. The reasons for this are (i) the long wavelengths involved, (ii) the need to measure away from the disturbing effects of the vessel, and (iii) the

Corresponding author address: Dr. Michael Richard Belmont, School of Engineering, Computer Science and Math, University of Exeter, EX4 5EB Exeter, United Kingdom.
E-mail: m.r.Belmont@exeter.ac.uk

DOI: 10.1175/JTECH2032.1

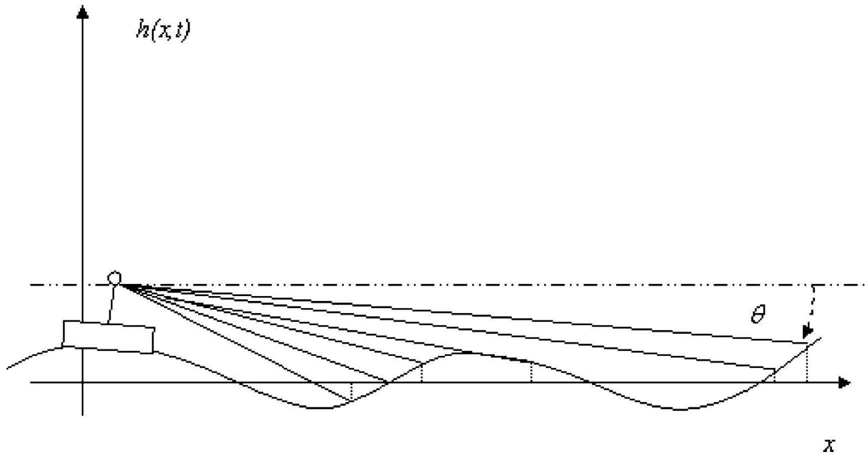

FIG. 1. Schematic of a vessel-mounted remote sensing beam scanning over the surface of a wave profile.

practical limits to the height of the equipment. The shallow operating angles mean that the basic lobe width of the illuminating beam, and hence the spatial resolution, at an angle θ is geometrically magnified by a factor $1/\tan\theta$ at the sea surface and, consequently, even for millimetric radar systems with large synthetic aperture arrays, the resolution achievable is unacceptably poor. Equally, when measuring surf or swash zone waves, very high resolution is required that is far beyond capabilities of such radars at even a modest range and normal incidence. The only systems capable of making desired shallow angle measurements at high resolution are lidars based upon coherent visible light sources.

Lidars (optical radars) were first developed as airborne surveying systems for coastal bathymetry and later for underwater obstacle detection (Casey et al. 1985; Steinvall et al. 1993, 1996; Nairn 1994; Armstrong et al. 1996; Guenther et al. 1996a,b; Lillycrop et al. 1996; Pope et al. 1997; West et al. 1999). They were based around the green 532-nm wavelength that was chosen for bottom echo generation because this spectral region corresponds to minimum absorption in particle-free seawater. To accurately determine the sea surface location bathymetry, lidars typically also employ a red beam, which is why such instruments are capable of providing sea surface profile data.

Despite being minimally absorbed by bulk seawater, green wavelengths are significantly scattered by components of calcareous plankton in the surface layers of the sea (Ivanov et al. 1986). The probe beams employed in airborne lidar systems typically operate at or near normal incidence where plankton scattering constitutes an unwanted return signal. However, for a vessel-mounted or portable shore-based system operating close to grazing incidence, this light scattering process will constitute an important data source. Other sources of backscatter are capillary waves, small local trochoidal wavelets, suspensions, and foam. As foam is a strong scattering agent, it means that the amplitude data can be used to identify those regions of the wave profile where the wave is breaking.

The signal returns from airborne lidars, at approximately normal incidence, are strong compared to the very weak returns available from the shallow angle lidars needed for coastal or shipborne operations. This problem is aggravated by the legal requirements for lidars to be eye safe, which obviates the use of the giant pulse lasers that have been employed in a wide field-of-view work wave roughness studies (Ivanov et al. 1986) and more recently using Raman scattering (Maslov et al. 2000). The consequential signal-to-noise ratio problem is one of the main reasons why such instruments have not been developed up until now. An overview of the innovative features of the system follows.

2. System overview

The basic principles of the shallow angle lidar are essentially the same as more traditional near-normal-incidence time of flight systems. The key new metrology features are the nonuniformly sampled character of the data and the very low signal-to-noise ratios. The latter requires the smallest practical field of view to minimize background illumination and this coupled with the need to scan over significant distances enforces the use of a monostatic approach. A standard prism-based polarization beam splitter was used to separate, transmit, and receive paths with the outgoing light being vertically polarized. The field of view employed was 0.1 mrad.

The present relatively low power system has a maximum range of approximately 200 m dependent upon conditions and employs a 532-nm wavelength light source with a pulse rate of 20 kHz and a half-width of 0.8 ns. The laser energy output per pulse was 10 μJ with a peak power of 8.33 kW. The collecting/transmitting optical element was a refracting lens of 0.15-m aperture with 1.2-m focal length. Thus, the basis of the resulting monostatic optical system is very similar to that employed by Duck et al. (2000) in the Haystack lidar.

The signal was acquired via a standard avalanche photodiode (APD) and wideband transconductance stage followed by an analog to digital capable of capturing data continuously at 4G samples per second. The present scanning is a single-axis line scan system using a low-inertia front surface mirror and a high-acceleration servo achieving a 50-sample scan over 200 m in 0.2 s. This allows line scans. This will be extended to a dual-axis system allowing multidirectional sets of line scans.

The key innovation that makes the shallow angle wave lidar feasible is the combination of the short pulse width/high repetition rate and the sophisticated signal processing system. The captured digitized signal return sequences were typically processed in real time but were also stored for additional postprocessing if required. The data presented here are all based upon real-time processing (as evident by occasional glitches). The wave height estimator is a multialgorithm real-time intelligent system with signal-to-noise ratio–based decision making. There is clearly a data acquisition rate versus processing cost trade-off, so fast simple thresholding is used for the larger amplitude near signals while more expensive adaptive cross-correlation methods are employed for remote return sequences of poor signal-to-noise ratio.

All detection techniques use a variable length N-point discrete time series of up to 400 samples of the return signals time history recorded at each laser pulse within a tracking time window. The windows center and length were initially set by the scan angle/distance with additional adaption based upon data history at poor signal-to-noise ratios. Typically, several tens of estimates of independent measurements of wave height were made at each scan point for averaging purposes. The exact number of samples N varies with the number of averages, the number of samples used per scan, and the range. In cross-correlation mode, two methods are possible. In what was termed the direct correlation method, the signal time series, $f_{\mathrm{sig}}(k)$, $k = 1, \ldots, N,$ was typically cross correlated with a "cleaned up" time signature $f_{\mathrm{ref}}(k)$, obtained from larger amplitude near returns (suitably transformed for the local incidence and wave slope). For offline work a more expensive parameterized refraction/scattering model of the signal return could be used for $f_{\mathrm{ref}}(k)$. In addition to zeroth-order wave profile estimates, this method also used parameters derived from intensity and time profile data acquired from clean near signals to model the prevailing scattering mechanisms.

An alternative to the direct correlation option was to cross correlate $f_{\mathrm{sig}}(k)$ with sequences from successive pulse measurements and sample locations. The direct method provides absolute times while the second approach gives incremental values between scan points that must be integrated up to determine out/back time.

In addition, the location of the peak of the cross-correlation function $R_{\mathrm{sig,ref}}(n)$ (and hence the signal out and back time) was estimated by least squares fitting a local M parameter analytic model of the maximum of $R_{\mathrm{sig,ref}}(n)$. This improves the sample variance/resolution by a further factor $\sqrt{M}$ over and above the standard sample variance/resolution gain provided by N-point cross correlation (Lee 1960). In real time, work processing costs restricted M to 4.

Given the use of a tracking window and previous data it is possible to make a good initial guess at the location of the correlation maximum, which avoids having to compute the redundant correlation tails at large shift values. This makes direct computation of the cross-correlation function, $R_{\mathrm{sig,ref}}(n)$, via $R_{\mathrm{sig,ref}}(n) = (1/N)\Sigma_{k=1}^{N} f_{\mathrm{sig}}(k) f_{\mathrm{ref}}(k + n)$, the preferred computational cost choice over the more standard FFT $\rightarrow$ complex conjugate multiplication $\rightarrow$ IFFT-based approach with its need for $N = 2^p$ points and the necessity to check for fold over errors, etc. (Brigham 1988).

3. Lidar operating modes

The lidar was designed to operate in a variety of modes. The fixed time mode entails essentially repetitively taking a one-dimensional snapshot of the sea surface spatial profile. This comprises a set of measurements of the surface elevation, $h(x, y, t)$, recorded at R sample locations in a total time, δt, which is short compared to that during which significant change, ε_h, in the surface profile occurs [i.e., $(\partial h(x, y, t)/\partial t)|_{\max}\delta t \leq \varepsilon_h$]. The instrument developed has a sufficiently high measurement rate so as to allow continuous *spatial movies* (i.e., a set of profiles recorded over the same region of space at a fixed time interval apart), thus providing information about the spatial dispersion behavior. The largest allowable distance between samples is set by the spatial generalized Nyquist requirement and the existing equipment has a range of up to 200 m depending upon the prevailing conditions and elevation.

Illustrative data are presented in Fig. 2, which shows

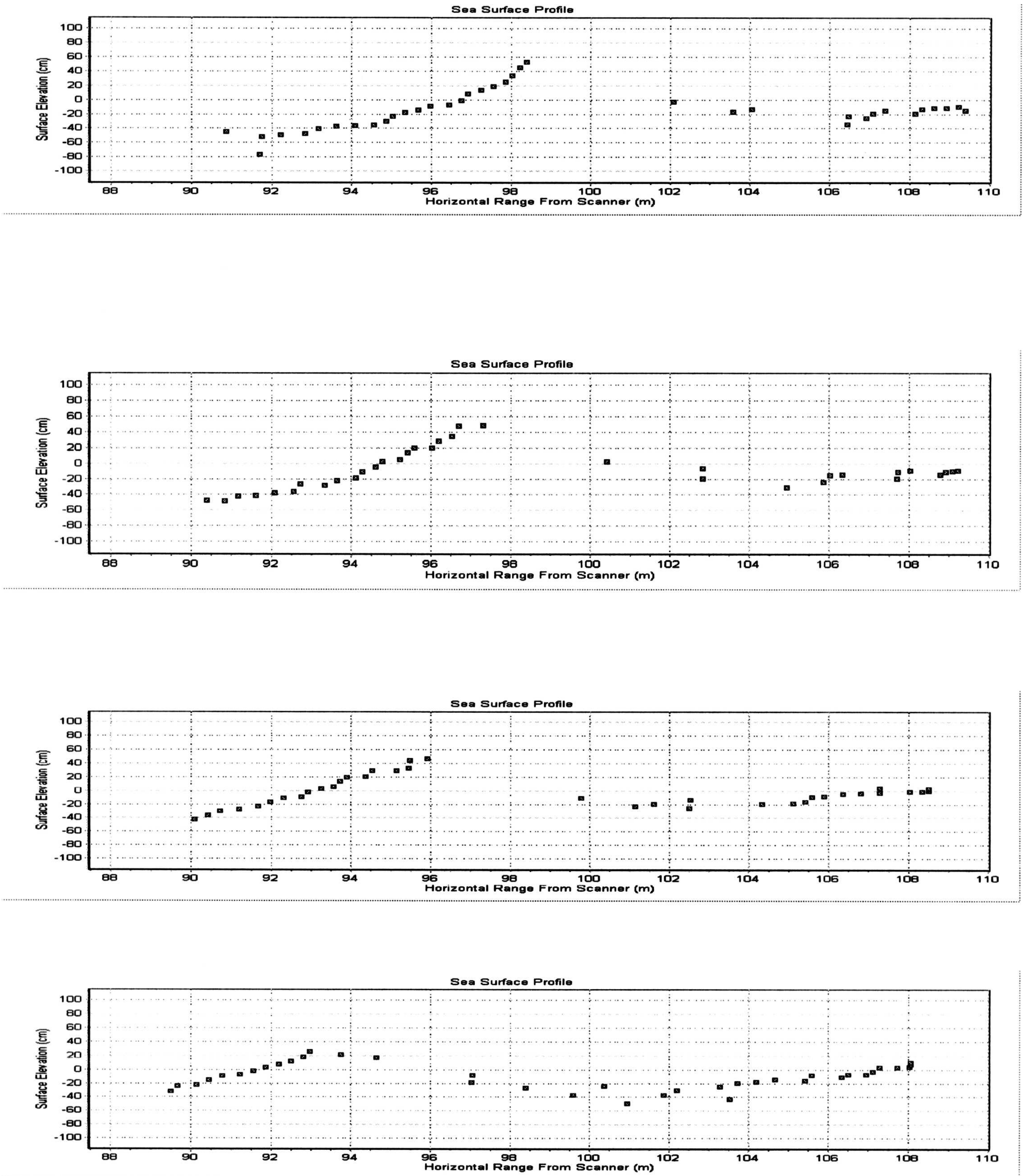

FIG. 2. Four successive frames taken from a "spatial wave movie" of a low-amplitude asymmetric wave propagating in shallow water.

four successive frames from a spatial movie of a small-amplitude ($\approx \pm$ 0.5 m), highly asymmetric wave in shallow water. The values in Fig. 2 are raw real-time wave height estimates (with no postprocessing) as evidenced by the presence of a small number of aberrant points. Under the prevailing conditions as indicated in the subsequent section dealing with validation, the vertical resolution was approximately $\pm$0.05 m.

The simplest fixed point mode operates with the beam at a fixed angle and partially mimics one or more traditional wave height sensors. It records the time evolution of surface elevation at a modest number of nominally fixed locations.

In this and the more general mixed space–time modes, the observation interval per individual wave height measurement is R times longer than in fixed time, with each measurement being allowed up to δt s. Furthermore, at shallow angles the nonuniformity effects mean that the sample locations change somewhat from sample to sample. If this change is unacceptably large, then the fixed point mode can only be employed when it is legitimate to use a sea model to extract the profile parameters. In such cases, the measurements are in fact in a mixed space–time mode.

The more general case of the mixed space–time mode is when the beam is scanned while allowing significant time between measurements. As in the fixed point mode, each individual wave height observation is allowed up to δt s rather than the allotment for a full scan. The data provided by the mixed space–time mode are less convenient than the snapshots, for as stated previously, it requires the use of a sea model to extract profiles. However, the signal-to-noise ratio and thus the maximum range is typically better. This is because the R-fold increase in observation time per sample allows up to R times more measurements to be averaged at each location than in the fixed time mode. Hence the sample standard deviation is reduced by a factor of $\sqrt{R}$. This consequently allows increased range in fixed time.

4. Geometric issues associated with shallow angle lidar

There are special issues associated with shallow angle lidars that can be seen in reference to Fig. 1. The major new metrology aspect is that the wave height values are inevitably nonuniformly distributed in space. The effect is clearly visible in Fig. 2, which shows a closer spacing of sample points on the front wave faces than on the rear. The most extreme case is when the rear wave slope locally exceeds the beam angle at which point wave shadowing occurs, as can be seen just beyond the wave top in Fig. 2.

Nonuniform sampling is inconvenient, as many data analysis algorithms, such as used in discrete spectral techniques, require uniform sample steps. However, if providing high spatial data rates is possible, well above the Nyquist limit, then the nonuniform sampling can be readily remapped to uniform using simple local interpolation methods. However, to achieve maximum range in any given mode, the total amount of collected light (and hence time spent) at each sample location should be as long as possible. Thus, there is a sound reason for operating at the minimum number of samples (hence maximum sample spacing) allowed by the generalized Nyquist condition. Under such circumstances, nonuniform to uniform remapping requires the use of Lagrangian interpolation methods (Marvasti 2001), which can be computationally expensive. This has thus led to the development of specialist signal processing techniques (Belmont 1993, 1995) for use with shallow angle lidars.

The wave shadow limit of nonuniformity would appear to be a significant difficulty. However, this missing data problem has been the subject of much work in the area of telecommunications, and provided the overall dataset is on average within the Nyquist limit, then subject to certain technical restrictions it is possible to reconstruct missing sections of such band-limited data (Feichtinger and Groechenig 1992; Marvasti 2001). While these regenerated points clearly do not contribute new information, and are linearly dependent on the original data, they can help considerably with the numerical sensitivity of certain processing algorithms as well as with rendering the data more directly accessible to users.

5. Validation

The lidar was extensively tested over solid surfaces and found to achieve the expected resolution range from ± 0.025 to ± 0.05 m depending upon the detection mode employed. For sea wave measurement, the lidar was validated against a conventional capacitance wave probe at a fixed location off a coastal jetty that was 6.5 m above sea level at the time of the measurements. Each wave height estimate was made from time series comprising 120 samples 0.5 ns apart. Wave height values were recorded at times 0.2 s apart. The final wave height at each time sample was taken as the average of 50 individual measurements. The raw data comparison is presented in Fig. 3 together with a difference histogram in Fig. 4.

The chosen conditions for validation tests involved low-amplitude, symmetrical waves of relatively long period waves, and a steeper angle (11° to the horizontal) was used than would normally be the case (the fixed time mode data in Fig. 2 were recorded at 5° to the horizontal). The first reason for these choices was that the small-amplitude waves very directly provide an indication of the vertical resolution of the lidar. Second, a combination of the small wave slope and the steeper incidence conditions minimized the wave profile–

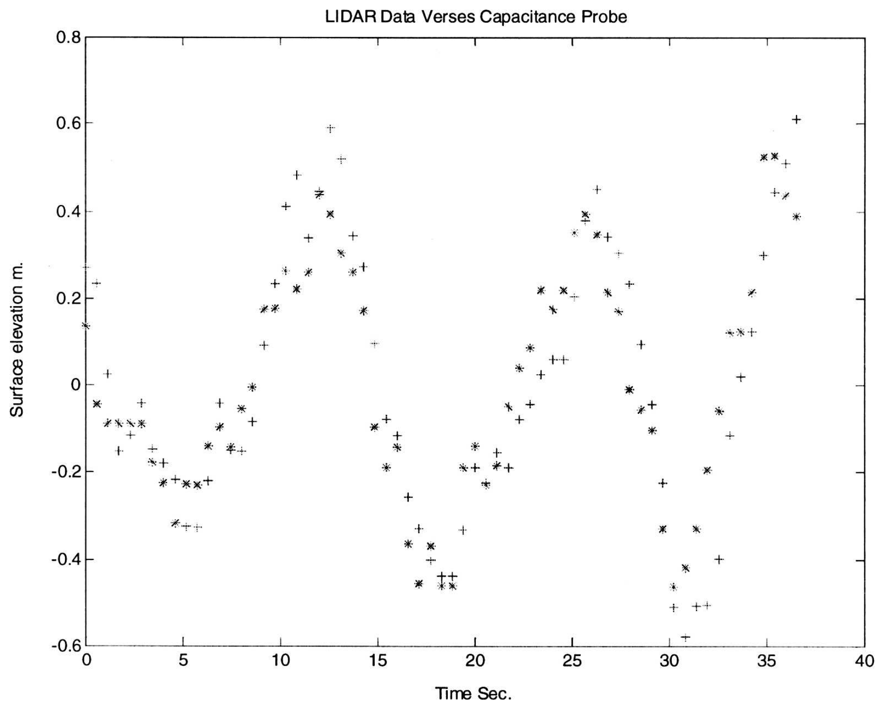

FIG. 3. Validation of lidar on small-amplitude waves at a fixed location using a standard capacitance wave probe. The cross symbols are the lidar and the stars are the capacitance probe.

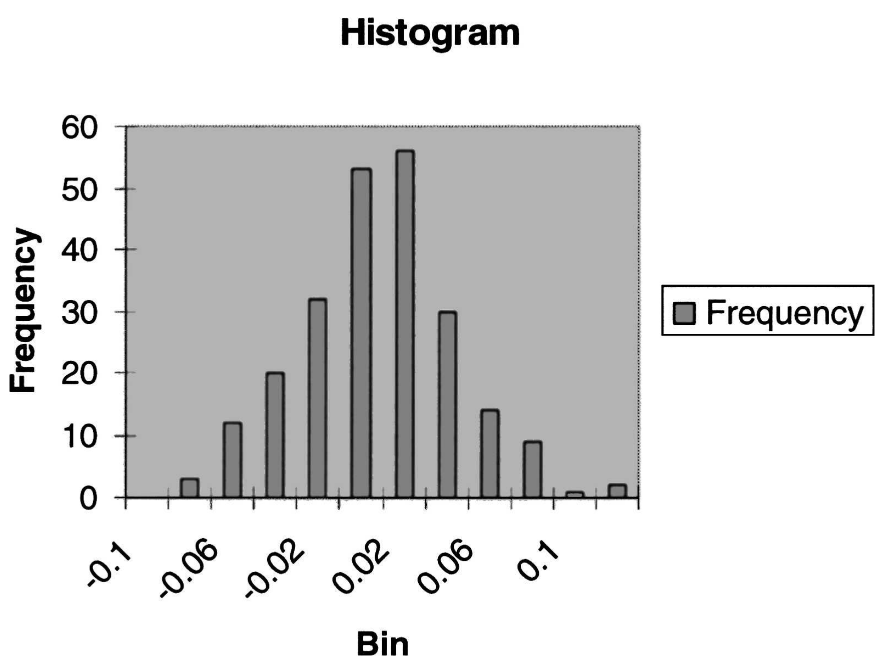

FIG. 4. A histogram showing the difference between the lidar with a capacitance wave probe made for small-amplitude waves, of rms value 0.36 m, and the lidar beam at a fixed angle of 11° to the horizontal. The bin units are in meters and the resulting standard deviation of the difference is 0.037 m.

induced displacement (the mixed space–time mode nonuniform sampling effect) of the lidar beam from the capacitance probe location. The worst-case shift between sample locations was estimated to be on the order of ±0.1 m.

In laboratory tests the capacitance probe was capable of resolving approximately 0.02 m under steady-state conditions but did show some evidence of the residual wetting lag effects to the same level of uncertainty during step response tests. The results presented in Fig. 4 show an rms difference of 0.037 m between the instruments for waves of rms amplitude 0.36 m, which given the additional measurements from land-based results and the sea data from Fig. 2 suggest that ± 0.05 m is a reasonable estimate of the vertical resolution.

REFERENCES

Armstrong, A., L. C. Huff, and G. F. Glang, 1996: New technology for shallow water hydrographic surveys. *Proc. 25th Joint Meeting of UJNR Sea-Bottom Surveys Panel,* San Francisco, CA.

Belmont, M. R., 1993: Nonuniform sampling specially for finite length data. *IEE Proc. F: Radar Signal Process.,* **140,** 55–62.

——, 1995: An extension to Nyquist's theorem for nonuniformly sampled finite length data. *Int. J. Adapt. Control Signal Process.,* **9,** 163–181.

Brigham, O. E., 1988: *The Fast Fourier Transform and Its Applications.* Prentice Hall, 448 pp.

Casey, M. J., R. A. O'Neil, and P. Conrad, 1985: The advent of Larsen. *Proc. Canadian Hydrographic Conf.,* Halifax, NS, Canada, Canadian Hydrographic Service, 7–12.

Clauss, G. F., 2001: *Synthesis of Deterministic Rogue Waves in Extreme Seas. Design and Operation for Abnormal Conditions II.* RINA.

Cote, L. J., and Coauthors, 1960: The directional spectrum of a wind generated sea as obtained from data obtained by the Stereo Wave Observation Project. NYU College of Engineering Meteorological Papers, Vol. 2, 88 pp.

Duck, T. J., D. P. Sipler, J. E. Salah, and J. W. Meriwether, 2000: Monostatic lidar at f/200: A new instrument at Millstone Hill/MIT Haystack Observatory. *Advances in Laser Remote Sensing,* A. Dabas et al., Eds., Ecole Polytechnique, 73–76.

Feichtinger, H. G., and K. Groechenig, 1992: Iterative reconstruction of multi-variate band-limited functions from irregular sampling values. *SIAM J. Math. Anal.,* **23,** 244–261.

Gallagher, E. J., S. Elgar, and R. T. Guzt, 1998: Observation of sand bar evolution on a natural beech. *J. Geophys. Res.,* **103** (C2), 3200–3215.

Guenther, G. C., T. J. Eisler, J. L. Riley, and S. W. Perez, 1996a: Obstruction detection and data decimation for airborne laser hydrography. *Proc. Canadian Hydrographic Conf.*, Halifax, NS, Canada.

——, R. W. L. Thomas, and P. E. LaRocque, 1996b: Design considerations for achieving high accuracy with the SHOALS Bathymetric Lidar System. *SPIE: Laser Remote Sens. Nat. Waters Theory Pract.,* **2964,** 54–71.

Ivanov, A. P., A. P. Chaykovskiy, I. S. Khutko, and N. P. Vorobey, 1986: Investigation of backreflection coefficient of optical radiation from a sea surface for grazing incidence. *Izv. Acad. Sci. USSR, Atmos. Oceanic Phys.,* **22,** 579–584.

Jackson, N. L., 1999: Evaluation of criteria for predicting erosion and accretion on an estuarine sand bar, Delaware Bay, New Jersey. *Estuaries,* **27** (2A), 215–223.

Lee, G. H., R. J. Nicholls, and W. A. Bukemeir, 1998: Storm-driven variability of the beach-nearshore profile at Duck, North Carolina, U.S.A. *Mar. Geol.,* **148** (3–4), 163–177.

Lee, Y. W., 1960: *Statistical Theory of Communication.* J. Wiley & Sons, 509 pp.

Lillycrop, W. J., L. E. Parson, and J. L. Irish, 1996: Development and operation of the SHOALS Airborne Lidar Hydrographic System. *SPIE: Laser Remote Sens. Nat. Waters Theory Pract.,* **2964,** 26–37.

Marvasti, F. A., Ed., 2001: *Nonuniform Sampling: Theory and Practice.* Plenum, 924 pp.

Maslov, D. V., V. V. Fadeev, and A. I. Lyashenko, 2000: A shore-based lidar for coastal seawater monitoring. *Proc. Fourth Workshop on Lidar Remote Sensing of Land and Sea,* Dresden, Germany, EARSeL, 46–52.

Morris, E. L., H. K. Zienkiewicz, M. M. A. Pourzanjani, J. O. Flower, and M. R. Belmont, 1992: Techniques for sea-state prediction. *Proc. Second Int. Conf. on Maneuvering and Control of Marine Craft,* Southampton, United Kingdom, University of Southampton and UK Ministry of Defence, 547–571.

——, ——, and M. R. Belmont, 1998: Short-term forecasting of the sea-state. *Int. Shipbuilding Prog.,* **45,** 383–400.

Nairn, R. R., 1994: Royal Australian Navy Laser Airborne Depth Sounder, The First Year of Operations. *Int. Hydrograph. Rev.,* **134,** 109–119.

Pope, R. W., B. A. Reed, G. R. West, and W. J. Lillycrop, 1997: Use of an airborne laser depth sounding system in a complex shallow-water environment. *Proc. Hydrographic Symp. and 15th Int. Hydro Conf.,* Monaco, Spain.

Steinvall, O., K. Koppari, and U. Karlsson, 1993: Experimental evaluation of an airborne depth-sounding lidar. *Opt. Eng.,* **32,** 1307–1321.

——, ——, U. Lejdebrink, J. Winell, M. Nilsson, R. Ellsen, and E. Gjellan, 1996: Depth sounding lidar: performance and models. *Laser Radar Technology and Applications,* Vol. 2748, G. W. Kamerman, Ed., SPIE, 18–38.

Tucker, M. J., 1991: *Waves in Ocean Engineering: Measurement, Analysis, Interpretation.* Ellis Horwood, 431 pp.

West, G. R., T. Graham, K. Smith, and J. Spittal, 1999: Improving the efficiency, safety and economy of the New Zealand National Charting Programme through the integrated use of Lidar in a multi-sensor survey. *Proc. U.S. Hydrographic Conf.,* Mobile, AL.